

Magnetic Fluffy Dark Matter

Kunal Kumar^a, Arjun Menon^{b,c}, Tim M.P. Tait^{d,e}

^a*Department of Physics and Astronomy, Northwestern University, Evanston, IL 60208*

^b*Physics Division, Illinois Institute of Technology, Chicago, IL 60616, USA*

^c*Institute of Theoretical Sciences, University of Oregon, Eugene, OR 97401, USA*

^d*Department of Physics and Astronomy, University of California, Irvine, CA 92697*

^e*Kavli Institute for Theoretical Physics, University of California, Santa Barbara, CA 93106, USA*

November 2, 2018

Abstract

We explore extensions of inelastic Dark Matter and Magnetic inelastic Dark Matter where the WIMP can scatter to a tower of heavier states. We assume a WIMP mass $m_\chi \sim \mathcal{O}(1 - 100)$ GeV and a constant splitting between successive states $\delta \sim \mathcal{O}(1 - 100)$ keV. For the spin-independent scattering scenario we find that the direct experiments CDMS and XENON strongly constrain most of the DAMA/LIBRA preferred parameter space, while for WIMPs that interact with nuclei via their magnetic moment a region of parameter space corresponding to $m_\chi \sim 11$ GeV and $\delta < 15$ keV is allowed by all the present direct detection constraints.

1 Introduction

The nature of dark matter is one of the fundamental questions facing physics, with numerous experiments being performed to search for it both directly and indirectly. Direct detection experiments hope to detect Weakly Interacting Massive Particles (WIMPs) by observing the recoil of target nuclei which interact with ambient WIMPs in the nearby galactic halo. One particular approach boils down to a counting experiment, looking for a signal in excess of all known background processes. Due to the expected small scattering cross-sections involved, these experiments typically need to reject many large backgrounds such as natural radioactivity and cosmic rays in order to be sensitive to dark matter scattering.

Another approach to direct detection of dark matter relies on the relative motion of the Earth through the dark matter halo. As the Earth orbits the Sun, which in turn is moving about the center of the Milky Way, the flux of WIMPs impinging on the Earth undergoes an annual modulation [1]. In particular, it is more likely to find WIMPs at high relative speeds when the Earth's motion is aligned with the Sun's (in the summer) than when they are pointing in opposite directions. A larger relative speed results in an increased potential for higher energy nuclear recoils. Given the finite energy thresholds of direct detection experiments, the result translates directly into an annual modulation of the rate of WIMP scattering with target nuclei. This modulation helps isolate a WIMP signal from the known backgrounds, which are not expected to display a strong modulation, and allows for detection of WIMPs without having to identify individual events as arising from signal or background. In fact, the DAMA/LIBRA experiment has reported evidence for just such an annual modulation signal whose peak is in June, consistent with the expectations of dark matter scattering [2]. However, in the simplest dark matter models the typical cross-sections needed to generate a modulation signal large enough so as to explain the DAMA/LIBRA results are so large that they are inconsistent with the null results at other direct detection experiments, including XENON100 [3] and CDMS II [4].

Inelastic Dark Matter (iDM) [5, 6] models attempt to resolve this puzzle. iDM models alleviate direct detection experimental constraints by requiring inelastic scattering of the form

$$\chi + N \rightarrow \chi^* + N \quad (1)$$

where χ is the incoming WIMP, χ^* is a heavier state into which it must scatter when interacting with a target nucleus N . Only scattering which transfers at least energy $\delta = m_{\chi^*} - m_{\chi}$ is kinematically allowed, which gives more relative weight to large velocity scattering, enhancing the annual modulation effect. In addition, since the momentum transfer of the scattering is controlled in part by the target mass (assuming it is not much greater than m_{χ}), the scattering rate is also different for different mass target nuclei. Initially, for $m_{\chi} \sim 100$ GeV and $\delta \sim 100$ keV, iDM models were able to explain the DAMA/Libra observations, while not being ruled out by other experiments. In the time since they were proposed, the increases in sensitivity have since closed the window of parameter space which could explain DAMA. For example, XENON100 has ruled out the iDM parameter space with a $\delta \lesssim 120$ keV that explains DAMA as scattering off of Iodine at the 90% confidence level [7, 8, 9].

In addition to its atomic mass number, another feature which distinguishes target nuclei are their electromagnetic properties, including charge and magnetic moment. Magnetic inelastic Dark Matter (MiDM) [10] exploits these differences by positing an inelastic WIMP whose primary interaction portal with Standard Model (SM) particles is by exchanging photons by virtue of a magnetic dipole moment [11, 12, 13, 14, 15]. Such a photonic portal favors target nuclei with larger charge and/or magnetic moment, and leads to an enhanced rate at DAMA, as compared to CDMS (for example) since Sodium and Iodine have high magnetic dipole moments in comparison to Germanium (see Table 1). A viable MiDM parameter space results [10, 16], subject to mild (and somewhat model-dependent) constraints from the null results of the Fermi/GLAST search for gamma-ray lines [17] from WIMP annihilation [18] and from LEP searches [19] for missing momentum [12, 20, 21].

Aesthetically, the need for a small splitting δ relative to other mass scales in the theory such as m_χ is somewhat mysterious. The existence of such a splitting may be motivated by introducing a weakly broken symmetry [10, 22, 23] which would otherwise require the elements of a WIMP multiplet to be degenerate, or can be produced in models where the WIMP is a composite state, bound either by a confined [24, 25] or by a weak long range force [26]. Such models naturally accommodate multiple mass scales, but it remains true that one tunes a parameter in order to generate a fine or hyper-fine splitting of the correct size to generate a realistic iDM model.

In this article, we explore a variation of composite inelastic models with a new feature ameliorating the need to tune any parameter related to δ . We consider a class of models in which the WIMP is a bound state of a new confined gauge force, where the dark matter is the lowest lying state consisting of a heavy preon which provides the bulk of the WIMP mass (and perhaps “flavor” quantum numbers which insure its stability), as well as some other light fundamental degrees of freedom. The confinement scale Λ of the new gauge sector satisfies $\Lambda \ll m_\chi$, such that one can expect a continuum of excited states whose levels are much smaller than the WIMP mass itself. Λ is also much smaller than the typical scale required of iDM in order to explain the DAMA results. The collective up-scattering from ground state into a variety of the excited states will explain the DAMA modulation results, with the characteristic splitting scale emerging organically from a theory whose characteristic splittings are somewhat smaller. Since this dark matter candidate looks something like a massive preon surrounded by a rather flimsy (easily perturbed) gluosphere, we refer to it as “fluffy” dark matter (fDM).

We assess the conditions under which fluffy dark matter can fit the DAMA modulation signal by interacting with nucleons either through a (canonical) Higgs-like portal, or by virtue of a magnetic moment through the photon portal. We model the fluffy spectrum as consisting of a ground state with a continuum of excited states at roughly evenly spaced intervals above it. As we will see shortly, the upshot is that the Higgs-like portal is ruled out by a combination of XENON100 [7] and low threshold CDMS [27] data, but magnetic fluffy dark matter (MfDM) is viable for WIMP masses around $m_\chi \sim 11$ GeV and $\delta \sim$ keV.

2 Effective Theories of Fluffy Dark Matter

Fluffy dark matter can arise as the low energy limit of a variety of UV theories. While it would be interesting to pursue some detailed examples (allowing one to discuss collider signals, which could show features of unparticles [28] or a hidden valley models [29]), we defer construction of detailed models to future work. Instead, we focus on the low energy dynamics, which we express in terms of an effective field theory containing the composite bound states.

As an underlying picture, we imagine a large N confining gauge theory, with confinement scale Λ . We refer to the vector bosons associated with the new gauge sector as “gluons” (without confusion with respect to the force carriers of the $SU(3)_c$ of the SM). There are also matter fields consisting of a heavy adjoint Majorana fermion (the “gluino”) which is a singlet under the SM gauge interactions, as well as some connector fields with both SM gauge quantum numbers, and transforming under the new force such that they can mediate interactions between bound states of the new gauge force and either the SM Higgs or photon by inducing a magnetic moment. It would be interesting to explore candidate models in terms of RS-like dual theories [30], but we leave such constructions for future work.

The lowest lying states of the confined sector consist of glueballs with masses of order Λ (which typically can decay into SM particles) and glueballinos, χ_i , Majorana fermion bound states of gluinos and gluons. We assume an underlying flavor symmetry which renders the gluino, and thus the χ_i , stable. The WIMP is identified as the lightest of these states with mass m_χ , and there is a sector of excited states with masses larger by order Λ . We will assume that the spectrum of excited states consists of a tower of states labelled by an integers n with masses,

$$m_n = m_\chi + n \delta \tag{2}$$

where $\delta \sim \Lambda \ll m_\chi$.

The connector fields are responsible for inducing interactions between the bound state WIMPs and the SM fields. One such interaction is a scalar coupling to two Higgs doublets,

$$r_\chi \bar{\chi}_i \chi_j H^\dagger H, \tag{3}$$

where H is the SM Higgs. After electroweak breaking, this leads to an interaction of $\bar{\chi}_i \chi_j$ with a single Higgs boson with strength $r_\chi v$. We have simplified the discussion by assuming that a single parameter r_χ controls the interaction, independent of i and j . In principle, this interaction can mediate elastic as well as inelastic scattering, but since we will find this case has difficulty explaining the DAMA results in the light of other null searches anyway, we will not dwell on this point here and just assume that something forbids the $i = j$ terms from occurring. We refer to a model coupled in this way as fluffy dark matter (fDM).

The second interaction we consider is a magnetic moment interaction,

$$\mu_\chi \bar{\chi}_i \sigma_{\mu\nu} \chi_j F^{\mu\nu}, \tag{4}$$

where μ_χ parameterizes the strength of the magnetic dipole, $\sigma_{\mu\nu} \equiv i[\gamma_\mu, \gamma_\nu]/2$, and $F^{\mu\nu}$ is the photon field strength. For a Majorana fermion, this interaction vanishes for $i = j$, which nicely explains why the WIMP should scatter inelastically off of nuclei. We have again made the simplifying assumption that the same parameter μ_χ at least approximately describes the strength of the interaction for all i and j . We refer to a fluffy WIMP which interacts with the SM primarily in this way as magnetic fluffy dark matter (MfDM).

3 Direct Detection of Fluffy Dark Matter

3.1 Dark Fluffy Scattering

3.1.1 fDM

For an inelastic scattering, the differential scattering rate may be written [31],

$$\frac{dR}{dE_R d\cos\gamma} = \frac{\kappa F^2(E_R)}{n(v_0, v_{\text{esc}})} \pi v_0^2 \left[\exp\left(-\frac{(\vec{v}_E \cdot \hat{v}_R + v_{\text{min}})}{v_0^2}\right) - \exp\frac{v_{\text{esc}}^2}{v_0^2} \right] \Theta(v_{\text{esc}} - |\vec{v}_E \cdot \hat{v}_R + v_{\text{min}}|) \quad (5)$$

where,

$$\kappa = N_T \frac{\rho_\chi}{m_\chi} \frac{\sigma_n m_N}{2\mu_n} \frac{(f_p Z + (A - Z)f_n)^2}{f_n^2}, \quad (6)$$

and N_T is the number of target nuclei per kilogram, ρ_χ is the local WIMP energy density, σ_n is the cross-section for scattering off a single nucleon, m_N is the nucleon mass, μ_n is the reduced mass of the nucleon-WIMP system, E_R is the recoil energy, $\cos\gamma$ is angle between the velocity of the earth and the recoil velocity of the nucleon as seen the earth's rest frame, $F^2(E_R)$ is the helm form factor describing the loss of coherence of the nucleus at large momentum transfer [32], $v_0 \simeq 220$ km/s is the WIMP velocity dispersion, $v_{\text{esc}} \simeq 500$ km/s is the escape velocity, \vec{v}_E is the velocity of the earth, and $n(v_0, v_{\text{esc}})$ normalizes the velocity distribution. We assume here a ‘‘standard’’ Maxwellian distribution of WIMP velocities in the halo. Conservation of energy and momentum dictate that the minimum velocity to scatter is,

$$v_{\text{min}} = \sqrt{\frac{1}{2m_N E_R}} \left(\frac{m_N E_R}{\mu} + \delta \right). \quad (7)$$

In the case of fDM, the Wimp scattering is into one of the whole tower of excited states. For a given final state excited WIMP j one has,

$$\kappa \rightarrow \kappa^j = N_T \frac{\rho_\chi}{m_\chi} \frac{\sigma_n^j m_N}{2\mu_n} \frac{(f_p Z + (A - Z)f_n)^2}{f_n^2}, \quad (8)$$

and ,

$$v_{\text{min}} \rightarrow v_{\text{min}}^j = \sqrt{\frac{1}{2m_N E_R}} \left(\frac{m_N E_R}{\mu} + \delta^j \right), \quad (9)$$

where as discussed above, we take $\delta^j \simeq j\delta$ and $\sigma_n^j \simeq \sigma_n$. This results in three relevant parameters controlling the predictions: the WIMP mass m_χ , the splitting between consecutive excited states δ , and the cross-section with nucleons σ_n .

3.1.2 MfDM

In MfDM scenarios the interactions between the WIMP and the target nucleus are mediated by photons which couple to the WIMP's magnetic dipole moment μ_χ . The interaction with the target nucleus can either proceed through its charge or magnetic moment, leading to both dipole - dipole (DD) and dipole-charge (DZ) interactions. The differential cross-section with respect to the recoil energy is,

$$\frac{d\sigma}{dE_R} = \sum_{i=1}^N \frac{d\sigma_{DZ}^i}{dE_R} + N \frac{d\sigma_{DD}}{dE_R} \quad (10)$$

$$\begin{aligned} \frac{d\sigma_{DZ}^i}{dE_R} = & \frac{4\pi Z^2 \alpha^2}{E_R} \left(\frac{\mu_\chi}{e}\right)^2 \left[1 - \frac{E_R}{v^2} \left(\frac{1}{2m_N} + \frac{1}{m_\chi}\right) \right. \\ & \left. - \frac{\delta^i}{v^2} \left(\frac{1}{\mu_{N\chi}} + \frac{\delta^i}{2m_N E_R}\right)\right] \left(\frac{S_\chi + 1}{3S_\chi}\right) F^2[E_R] \end{aligned} \quad (11)$$

$$\frac{d\sigma_{DD}}{dE_R} = \frac{16\pi\alpha^2 m_N}{v^2} \left(\frac{\mu_{nuc}}{e}\right)^2 \left(\frac{\mu_\chi}{e}\right)^2 \left(\frac{S_\chi + 1}{3S_\chi}\right) \left(\frac{S_N + 1}{3S_N}\right) F_D^2[E_R] \quad (12)$$

where N is the heaviest state kinematically accessible [10]. A list of values for Z and μ_n for a variety of relevant target nuclei is presented in Table 1. The DD term is proportional to μ_{nuc}^2 , implying that the rate at DAMA (whose target is NaI) can be significantly enhanced as compared to experiments using target nuclei with lower μ , such as xenon or germanium.

In Eqs. (10)-(12), $F^2[E_R]$ is the Helm form factor [32] and $F_D^2[E_R]$ is the nuclear magnetic dipole form-factor. While the helm form factor is expected to be a good approximation for the factor by which the cross section decreases for non-zero momentum transfer in spin independent interactions, the nuclear magnetic dipole moment form-factor deserves more careful treatment. The usual thin-shell model for spin-dependent interactions need not be a good approximation for heavier nuclei [33]. We follow Ref. [34] in obtaining the form factors for ^{129}Xe , ^{131}Xe , ^{133}Cs and ^{127}I . The theoretical model therein from which we have derived our form factor reproduces observables like magnetic moments of relevant nuclear states quite well. Nonetheless, as discussed in more detail in Ref. [10], this remains a source of uncertainty in our predictions which is difficult to quantify in the absence of more direct experimental inputs. We define the form factor as

$$F^2(E_r) = \frac{1}{N} \left(f_0^2 \Omega_0^2 F_{00}^2(E_r) + 2f_0 f_1 \Omega_0 \Omega_1 F_{01}(E_r) + f_1^2 \Omega_1^2 F_{11}^2(E_r) \right) \quad (13)$$

Isotope	Z	Abundance(%)	Spin	μ_{nuc}/μ_N
^{17}O	8	0.038	5/2	-1.894
^{19}F	9	100	1/2	2.629
^{23}Na	11	100	3/2	2.218
^{43}Ca	20	0.135	7/2	-1.317
^{73}Ge	32	7.76	9/2	-0.879
^{127}I	53	100	5/2	2.813
^{129}Xe	54	26.40	1/2	-0.778
^{131}Xe	54	21.23	3/2	+0.692
^{133}Cs	55	100	7/2	+2.582
^{183}W	74	14.31	1/2	+0.118

Table 1: Natural isotopes with quantities relevant to direct detection searches [36].

where Ω_0, Ω_1 are effective g factors (Table IV, Ref. [34]), and F_{00}, F_{01}, F_{11} are spin structure functions (Figs. 3-4, Ref. [34]). The coefficients $f_0 = \mu_n + \mu_p$ and $f_1 = \mu_p - \mu_n$ are the isoscalar and isovector coupling constants. $\mu_n = -1.9\mu_N$ and $\mu_p = 2.8\mu_N$ are magnetic moments of the proton and neutron. The overall factor N is fixed by imposing the condition that the form factor is 1 at zero momentum transfer.

For all other nuclei we use the distribution [35] which takes into account the coupling to all ‘odd-group’ nucleons ,

$$F^2(qr_n) = \begin{cases} j_0^2(qr_n) & (qr_n < 2.55, qr_n > 4.5) \\ 0.047 & (2.55 < qr_n < 4.5) \end{cases} . \quad (14)$$

3.2 Fits to the DAMA/LIBRA Signal

Our next task is to assess the ability of fDM and MfDM to fit the DAMA observations. We scan over m_χ and δ , and construct a χ^2 function to fit the amplitude over the 2 – 8 keVee energy bins reported by DAMA/LIBRA, using the quenching factors 0.3 (0.09) for Na (I) [37]. To construct the χ^2 -function, we estimate the modulated amplitude as half of the difference between the maximal and minimal scattering rates during the year¹. We focus on the 2 – 8 keVee region, since for higher energies both the observed and predicted spectra are consistent with zero modulation and the inclusion of these energy bins would act to artificially improve the quality of the fit.

For each point in the $m_\chi - \delta$ plane, we find the corresponding spin-independent scattering cross-section σ_n for fDM or the dipole moment μ_χ for MfDM that leads to the minimal value of χ^2 . The results are shown in Fig. 1. Using these values of σ_n for fDM and μ_χ for MfDM

¹This approximation breaks down if the scattering rate were to be zero for a substantial part of the winter months. However we find that this approximation is valid for all of the DAMA/LIBRA preferred regions of parameter space.

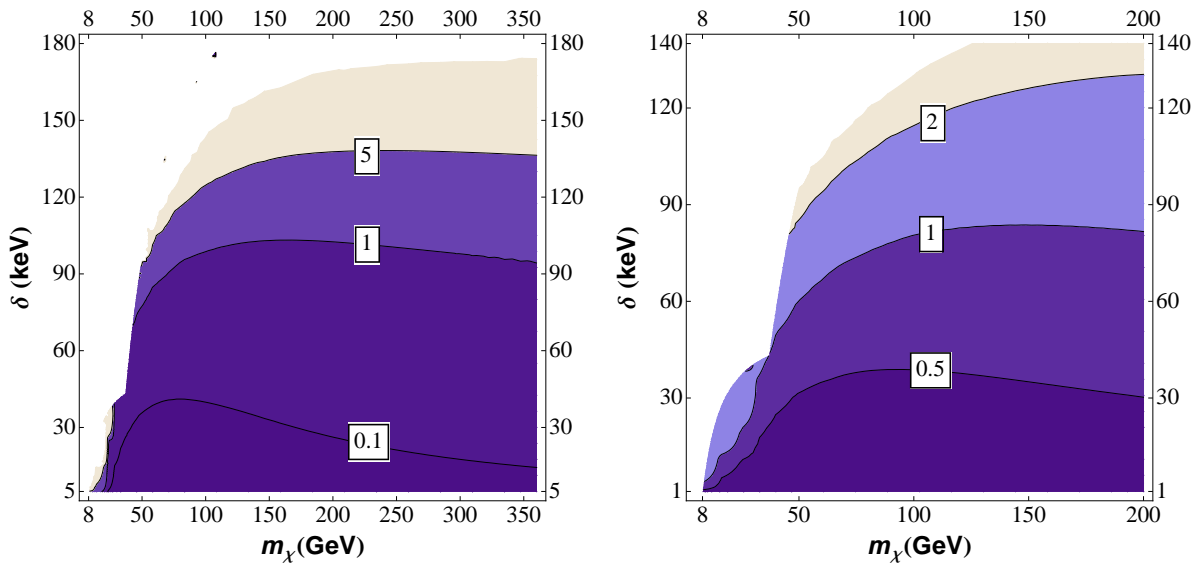


Figure 1: Best fit values of σ_n^0 in units of 10^{-40} cm^2 (left panel) in the fDM scenario and μ_χ in units of $10^{-3} \mu_N$ (right panel) in the MfDM scenario. The maximum value in both cases is along the edge of the tan (off-white) region and is 24 in the fDM case and 2.8 in the fDM case. The white region in both plots is not allowed as the δ is too high for any scattering to take place. The kink in the boundary of the allowed region at $m_\chi \sim 40$ GeV is due to the fact that below this mass the upper limit on δ is set by scattering off of Sodium, and above it the limit is set by scattering off of Iodine.

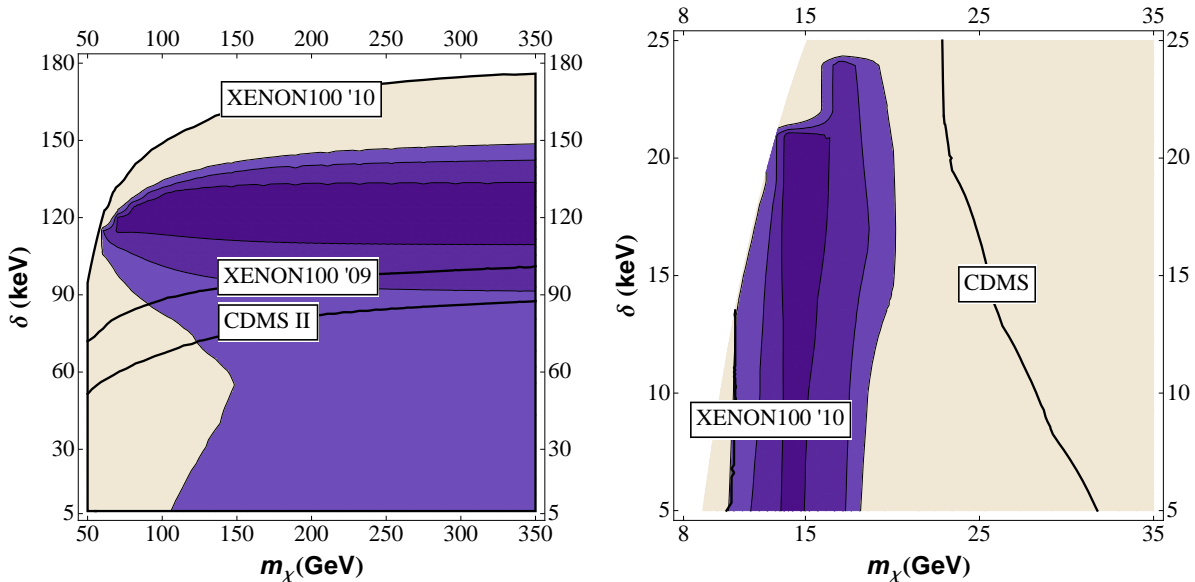


Figure 2: Constraints on fDM, for large (m_χ, δ) (left) and small (m_χ, δ) (right), from direct detection experiments. The darker blue (grey), blue (grey) and lighter blue (grey) regions correspond to the fDM points that fit the DAMA/LIBRA annual modulation spectrum at 68%, 95%, and 99.7% C.L. In the left panel regions to the right and below of each solid black line are ruled out by the corresponding direct detection experiment. In the panel on the right, parameter space to the left of the line corresponding to the CDMS low threshold limit and to the right of the line from XENON10 '10 are excluded.

we can calculate the scattering rates at a particular direct detection experiment using Eq.(5) and Eq.(10) respectively. In this sense, the bounds on regions of m_χ and δ that we later derive from other experiments are themselves dependent on DAMA. We consider bounds from XENON100 (both the 11.17 days of data collected in 2009 [38] and the 100 days of data collected in 2010 [3]); CDMS II (including the low energy threshold analysis) [4]; KIMS [39]; and COUPP [40]. Bounds from XENON10 [41], ZEPLIN III [42], CRESST II [43, 44], and PICASSO [45] were considered, but do not appear in the figures as they are weaker than the bounds from other experiments. A summary of the data used to constrain fDM and MfDM scenarios is presented in Table 2.

In the plane of m_χ and δ , we find islands where both fDM and MfDM can provide an acceptable fit within error bars to the DAMA/LIBRA data. We map out the contours of 68%, 95%, and 99.7% C.L. agreement with the DAMA/LIBRA annual modulation amplitude, which we plot as the darkest blue (grey), dark blue (grey), and lighter blue (grey) shaded regions of Fig. 2 and Fig. 3 for both fDM and MfDM, and for low mass and high mass WIMPs. These contours are somewhat conservative in the sense that the best fit points have $\chi^2 < 1$ per degree of freedom. The tan (off-white) regions of each plot have poorer agreement, and the white regions of each figure have δ large enough that $v_{\min} > v_{\text{esc}}$, so no scattering is possible.

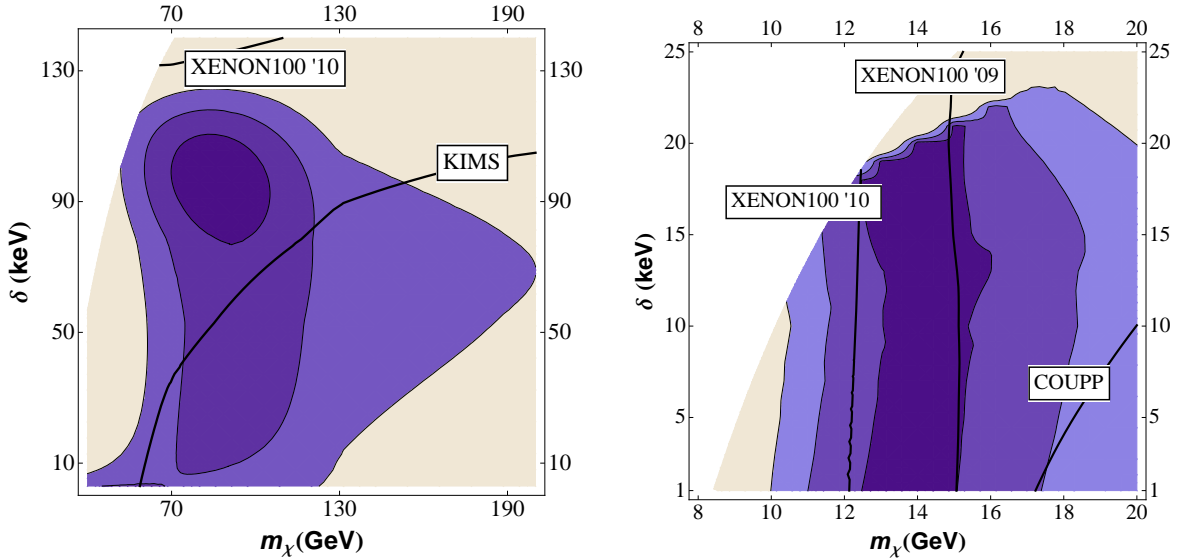


Figure 3: Constraints on MfDM, for large (m_χ, δ) (left) and small (m_χ, δ) (right), from direct detection experiments. The darker blue (grey), blue (grey) and lighter blue (grey) regions correspond to the MfDM points that fit the DAMA/LIBRA annual modulation spectrum at 68%, 95%, and 99.7% C.L. The parameter space below and to the right of each of the black lines are ruled out by the corresponding experiment.

3.2.1 fDM

In the case of fDM, the high WIMP mass region is shown in the left panel of Fig. 2. The regions that fit the DAMA/LIBRA data well are approximately the same as the those previously identified in Ref. [46, 47] as being preferred by iDM. As such, this parameter space represents a WIMP which is not particularly fluffy because only one excited state is relevant for the scattering. It thus suffers the same fate as standard iDM and is highly constrained by XENON100 and CDMS for a Maxwellian halo [9].

In the low mass region, there is a separate island of good fit region, where the scattering is dominantly off of Na nuclei. Here, we find roughly any $\delta \lesssim 20$ keV works to describe DAMA, which for small splitting looks very much like a fluffy WIMP. However, WIMP masses above around 11 GeV are excluded by XENON 100 (which is essentially enough to remove the interesting parameter space) and the CDMS low threshold analysis removes the entire interesting low mass region as well. It is interesting to note that unlike the other exclusion limits, the low threshold CDMS limit excludes the region to its left, for smaller m_χ . This is due to the fact that the values of σ_n extracted from fitting to DAMA/LIBRA increase as m_χ decreases, as can be seen in the left panel of Fig. 1, which compensates the smaller typical scattering energy all the way to the region where no scattering is possible.

Combining the low and high mass regions, we see that the regions of fDM parameter space consistent with the DAMA energy spectrum are strongly constrained by the null search limits from other direct detection experiments.

Experiment	Exposure	Time Period	Signal Window	Observed
CDMS '08	194.1 kgd	7/1/07 - 9/1/08	10 - 100 keV	2
CDMS Low-Energy	241 kgd	101/06 - 9/1/08	2 - 5 keV	324
XENON10	0.3×316.4 kgd	10/6/06 - 2/14/07	4.5 - 75 keV	13
XENON100	161 kgd	10/20/09 - 9/12/09	7.4 - 29.1 keV	0
XENON100	48×100.9 kgd	1/13/10 - 6/8/10	8.4 - 44.6 keV	3
ZEPLIN III	0.5×63.3 kgd	2/27/08 - 5/20/08	17.5 - 78.8 keV	5
CRESST II (W)	$0.59 \times 0.9 \times 48$ kgd	3/27/07 - 7/23/07	12 - 100 keV	7
CRESST(O)	564 kgd	7/09 - 10/10	~ 10 - 40 keV	32
CRESST(Ca,W,O)	730 kgd	7/09 - 3/11	~ 10 - 40 keV	67
KIMS	3409 kgd	1/05 - 12/06	20 - 100 keV	955
COUPP	28.1 kgd	11/19/09 - 12/18/09	21 - 200 keV	3
PICASSO	13.75 kgd	6/07 - 7/08	20 - 200 keV	2051

Table 2: Exposure and data collection period, signal energy window, and number of observed events at various dark matter direct detection experiments. For CRESST we write ~ 10 keV for the sake of brevity in the table. The threshold is different for each of their detector modules. The Observed events at KIMS has been inferred using the exposure and event rates from Ref. [39].

3.2.2 MfDM

The results for MfDM in the high WIMP mass range ($m_\chi \sim 100$ GeV) are shown in the left panel in Fig 3. The DAMA/LIBRA spectrum is well fit in the region $m_\chi \sim 80$ GeV and $\delta \sim 100$ keV. The strongest constraints obtained are from XENON100 and KIMS (whose Cs and I nuclei have relatively high nuclear magnetic moments, and are thus particularly good probes of MfDM). XENON100 sets the stronger constraint and excludes the entire region allowed by DAMA. Similarly to the fDM scenario, this region of parameter space does not correspond to a very fluffy WIMP and the region of parameter space favored by DAMA/LIBRA is similar to that found in the MiDM scenario of Ref. [10].

In the low WIMP mass region, we find that masses around 14 GeV and with $\delta \lesssim 20$ keV provide a good fit to DAMA. This region is shown in the right panel of Figure 3, where we see relevant constraints from XENON100 and COUPP. CDMS low threshold constraint is weak, due to the small magnetic coupling, while the XENON100 limit only constrains a part of the parameter space that provides a good fit to the DAMA/LIBRA data. The XENON100 limit allows a significant portion of the MfDM parameter space that fits the DAMA/LIBRA signal at the $> 95\%$ C.L. The fit in this allowed region is also not dependent on δ for values less than 15 keV.

The larger δ region indicates that MiDM with WIMP masses around 11 GeV is consistent with current direct detection data. The small δ region realizes the hope of a fluffy WIMP, with many excited states contributing to the scattering. For example, an 11 GeV WIMP

can scatter up to states that are heavier by $\lesssim 15$ keV, so for a splitting of $\delta = 1$ keV, 15 excited states participate in the scattering. For smaller values of δ , the number of relevant states in the scattering increases.

4 Outlook

We have considered a picture where dark matter is the lowest lying state in a composite sector, whose low energy scattering with nuclei is inelastic. We refer to such a WIMP as fluffy, since its internal structure as a confined state is rather easily perturbed by its environment. For very low confinement scales, the preferred inelastic splitting emerges somewhat organically, driven largely by the energy thresholds of DAMA itself. We perform fits and find that light (~ 11 GeV) WIMPs with small splittings δ provide the best fits to the DAMA observation of annual modulation and energy spectrum. For a WIMP whose interactions with the SM are through iso-spin conserving spin-independent couplings to the SM, constraints (largely from XENON 100) are enough to close off the region of parameter space able to explain the DAMA signal. However, a fluffy WIMP whose interactions are magnetic in nature can explain DAMA and still remain consistent with the bounds from other direct detection experiments. Because of the low masses favored by the fit, it is difficult for XENON to access the parameter space of interest. Lower threshold experiments perhaps offer the most promising probes in the future.

A low compositeness scale is a challenge for cosmology, and leads to potentially many unusual features for a theory of dark matter. To begin with, our analysis assumed the bulk of the WIMPs in the halo were in the ground state. If this were not the case, the WIMPs would down-scatter as well as up-scattering. One could imagine engineering this possibility directly into a model of luminous dark matter [48], which is an interesting independent line of investigation beyond the scope of this work, but we prefer to imagine there are interactions which efficiently de-excite the WIMPs, perhaps through a coupling to neutrinos [49].

In the early Universe, a fluffy WIMP can undergo a freeze-out process which differs substantially from a standard WIMP. The seed partons may freeze out at early times, but the confined states may come back into equilibrium because of the surrounding clouds of light partons increase their effective cross sections after the phase transition. This can lead to an additional dilution of the WIMPs at late times [50, 51, 52]. Alternately, one could explore the case where excitations with large splittings continue to play an active cosmological role, perhaps obviating the need for an external stabilization symmetry [53, 54].

Since we favor a low confinement scale, there will be additional (at least) gauge degrees of freedom contributing to the thermal bath even at relatively late times. Precision measurements of the primordial abundances of light elements produced through big bang nucleosynthesis, and of the cosmic microwave background, provide tight constraints on additional light degrees of freedom during the relevant epochs [55, 56]. Both sets of measurements are currently consistent with no new degrees of freedom being present, with error bars allowing for around at most one new state equivalent to an “effective neutrino species”. Future CMB measurements by PLANCK are expected to have the precision to shrink the uncertainties

to the order of a tenth of an effective neutrino species [57]. One could imagine evading these bounds if the dark sector has a separate temperature from the SM plasma [52], or if the coupling of the new confined force is time-dependent, perhaps being set by value of a modulus through a term such as $\phi F^{\mu\nu} F_{\mu\nu}$, where $\langle\phi\rangle$ starts at large values, leading to a tightly bound WIMP during the cosmologically sensitive times, but rolls to lower values in late cosmological times, leading to the WIMPs puffing up.

After confinement, one can expect the analogues of glueball states for the new gauge force (whose masses should be roughly $\Lambda \sim \text{keV}$) could contribute to relevant phenomena. For example, if sufficiently long-lived, they could end up as a subdominant component of warm dark matter, or their decays could contribute additional entropy to the Universe. In addition, such states may have large (strong force residual) interactions with the WIMPs. If WIMPs can efficiently lose kinetic energy in collisions, either by converting kinetic energy to excitation energy and then de-exciting by radiating a glueball, or by exchanging glueballs in elastic collisions, it can cause elliptical galaxies to become spherical [58, 59]. One can even imagine more radical shifts in galactic dynamics, such as cases where some fraction of the binding is due to glueball exchange (in addition to gravity), with the galaxy itself looking something like the analogue of a heavy nucleus state of the new gauge force.

One can imagine other scenarios in which a fluffy WIMP might provide an interesting model of dark matter. For example, models of exciting dark matter [60] invoke an MeV split excited WIMP to explain the INTEGRAL/SPI 511 keV gamma ray excess [61]. One could easily imagine a fluffy WIMP model allowing this small scale to emerge organically as it did here in an inelastic scattering context. It would be interesting to see if a common framework could potentially explain the DAMA signal as well as the INTEGRAL excess within a common framework relying on a single value of δ .

These potential features are interesting, and highlight both the challenges in designing a workable cosmology, as well as motivating explorations of some truly novel phenomena. While straw man constructions are easy to construct piece by piece, a compelling, unified framework would be worth pursuing. We leave a detailed exploration of these ideas for future work.

Acknowledgments

We are grateful for helpful conversations with Jonathan Feng and James Bjorken. TT is pleased to acknowledge the SLAC theory group for their hospitality during his many visits, and to the KITP (supported in part by the NSF under Grant No. PHY05-51164) where part of it was performed. The work of TT is supported in part by the NSF under grant PHY-0970171. AM was supported at IIT by DOE grant number DE-FG02-94ER40840 and at University of Oregon by DOE grant number DE-FG02-96ER40969.

References

- [1] A. K. Drukier, K. Freese, D. N. Spergel, Phys. Rev. **D33**, 3495-3508 (1986), K. Freese, J. A. Frieman, A. Gould, Phys. Rev. **D37**, 3388 (1988).
- [2] R. Bernabei *et al.* [DAMA Collaboration], Eur. Phys. J. **C56**, 333-355 (2008). [arXiv:0804.2741 [astro-ph]].
- [3] E. Aprile *et al.* [XENON100 Collaboration], [arXiv:1104.2549 [astro-ph.CO]].
- [4] Z. Ahmed *et al.* [The CDMS-II Collaboration], Science **327**, 1619 (2010) [arXiv:0912.3592 [astro-ph.CO]], Z. Ahmed *et al.* [CDMS-II Collaboration], Phys. Rev. Lett. **106**, 131302 (2011) [arXiv:1011.2482 [astro-ph.CO]].
- [5] D. Tucker-Smith, N. Weiner, Phys. Rev. **D64**, 043502 (2001). [hep-ph/0101138].
- [6] T. Han, R. Hempfling, Phys. Lett. **B415**, 161-169 (1997); L. J. Hall, T. Moroi and H. Murayama, Phys. Lett. B **424**, 305 (1998) [arXiv:hep-ph/9712515].
- [7] E. Aprile *et al.* [XENON100 Collaboration], Phys. Rev. D **84**, 061101 (2011) [arXiv:1104.3121 [astro-ph.CO]].
- [8] D. S. M. Alves, M. Lisanti, J. G. Wacker, Phys. Rev. **D82**, 031901 (2010). [arXiv:1005.5421 [hep-ph]].
- [9] M. Farina, M. Kadastik, D. Pappadopulo, J. Pata, M. Raidal and A. Strumia, Nucl. Phys. B **853**, 607 (2011) [arXiv:1104.3572 [hep-ph]].
- [10] S. Chang, N. Weiner, I. Yavin, Phys. Rev. **D82**, 125011 (2010). [arXiv:1007.4200 [hep-ph]].
- [11] J. Bagnasco, M. Dine, S. D. Thomas, Phys. Lett. **B320**, 99-104 (1994). [hep-ph/9310290].
- [12] K. Sigurdson, M. Doran, A. Kurylov, R. R. Caldwell, M. Kamionkowski, Phys. Rev. **D70**, 083501 (2004). [astro-ph/0406355].
- [13] V. Barger, W. -Y. Keung, D. Marfatia, Phys. Lett. **B696**, 74-78 (2011). [arXiv:1007.4345 [hep-ph]].
- [14] E. Masso, S. Mohanty, S. Rao, Phys. Rev. **D80**, 036009 (2009). [arXiv:0906.1979 [hep-ph]].
- [15] T. Banks, J. -F. Fortin, S. Thomas, [arXiv:1007.5515 [hep-ph]].
- [16] T. Lin and D. P. Finkbeiner, Phys. Rev. D **83**, 083510 (2011) [arXiv:1011.3052 [astro-ph.CO]].

- [17] A. A. Abdo *et al.*, Phys. Rev. Lett. **104**, 091302 (2010) [arXiv:1001.4836 [astro-ph.HE]].
- [18] J. Goodman, M. Ibe, A. Rajaraman, W. Shepherd, T. M. P. Tait and H. B. P. Yu, Nucl. Phys. B **844**, 55 (2011) [arXiv:1009.0008 [hep-ph]].
- [19] P. Achard *et al.* [L3 Collaboration], Phys. Lett. **B587**, 16-32 (2004). [hep-ex/0402002].
- [20] J. -F. Fortin, T. M. P. Tait, [arXiv:1103.3289 [hep-ph]].
- [21] P. J. Fox, R. Harnik, J. Kopp, Y. Tsai, Phys. Rev. **D84**, 014028 (2011). [arXiv:1103.0240 [hep-ph]].
- [22] N. Arkani-Hamed, D. P. Finkbeiner, T. R. Slatyer, N. Weiner, Phys. Rev. **D79**, 015014 (2009). [arXiv:0810.0713 [hep-ph]].
- [23] M. Pospelov and A. Ritz, Phys. Rev. D **78**, 055003 (2008) [arXiv:0803.2251 [hep-ph]].
- [24] D. S. M. Alves, S. R. Behbahani, P. Schuster, J. G. Wacker, Phys. Lett. **B692**, 323-326 (2010). [arXiv:0903.3945 [hep-ph]].
- [25] G. D. Kribs, T. S. Roy, J. Terning, K. M. Zurek, Phys. Rev. **D81**, 095001 (2010). [arXiv:0909.2034 [hep-ph]].
- [26] D. E. Kaplan, G. Z. Krnjaic, K. R. Rehermann and C. M. Wells, JCAP **1005**, 021 (2010) [arXiv:0909.0753 [hep-ph]].
- [27] Z. Ahmed *et al.* [CDMS-II Collaboration], Phys. Rev. Lett. **106**, 131302 (2011). [arXiv:1011.2482 [astro-ph.CO]].
- [28] H. Georgi, Phys. Rev. Lett. **98**, 221601 (2007). [hep-ph/0703260].
- [29] M. J. Strassler, K. M. Zurek, Phys. Lett. **B651**, 374-379 (2007). [hep-ph/0604261].
- [30] N. Arkani-Hamed, M. Porrati, L. Randall, JHEP **0108**, 017 (2001). [hep-th/0012148].
- [31] D. P. Finkbeiner, T. Lin and N. Weiner, Phys. Rev. D **80**, 115008 (2009) [arXiv:0906.0002 [astro-ph.CO]].
- [32] R. H. Helm, Phys. Rev. **104**, 1466 (1956).
- [33] J. Engel, S. Pittel, P. Vogel, Int. J. Mod. Phys. **E1**, 1-37 (1992).
- [34] P. Toivanen, M. Kortelainen, J. Suhonen, J. Toivanen, Phys. Rev. **C79**, 044302 (2009).
- [35] J.D. Lewin, P.F. Smith, Astropart. Phys.,**6**, 87-112 (1996).
- [36] D. Lide, CRC Handbook of Chemistry and Physics, 91st Edition.

- [37] R. Bernabei, P. Belli, V. Landoni, F. Montecchia, W. Di Nicolantonio, A. Incicchitti, D. Prosperi, C. Bacci *et al.*, Phys. Lett. **B389**, 757-766 (1996).
- [38] E. Aprile *et al.* [XENON100 Collaboration], Phys. Rev. Lett. **105**, 131302 (2010). [arXiv:1005.0380 [astro-ph.CO]].
- [39] H. S. Lee *et al.* [KIMS Collaboration], Phys. Rev. Lett. **99**, 091301 (2007) [arXiv:0704.0423 [astro-ph]].
- [40] E. Behnke, J. Behnke, S. J. Brice, D. Broemmelsiek, J. I. Collar, P. S. Cooper, M. Crisler, C. E. Dahl *et al.*, Phys. Rev. Lett. **106**, 021303 (2011). [arXiv:1008.3518 [astro-ph.CO]].
- [41] J. Angle *et al.* [XENON10 Collaboration], Phys. Rev. D **80**, 115005 (2009) [arXiv:0910.3698 [astro-ph.CO]].
- [42] D. Y. Akimov *et al.* [ZEPLIN-III Collaboration], Phys. Lett. B **692**, 180 (2010) [arXiv:1003.5626 [hep-ex]].
- [43] G. Angloher, M. Bauer, I. Bavykina, A. Bento, A. Brown, C. Bucci, C. Ciemniak, C. Coppi *et al.*, [arXiv:0809.1829 [astro-ph]].
- [44] G. Angloher, M. Bauer, I. Bavykina, A. Bento, C. Bucci, C. Ciemniak, G. Deuter, F. von Feilitzsch *et al.*, [arXiv:1109.0702 [astro-ph.CO]].
- [45] S. Archambault, F. Aubin, M. Auger, E. Behnke, B. Beltran, K. Clark, X. Dai, A. Davour *et al.*, Phys. Lett. **B682**, 185-192 (2009). [arXiv:0907.0307 [hep-ex]].
- [46] D. Tucker-Smith, N. Weiner, Phys. Rev. **D72**, 063509 (2005). [hep-ph/0402065].
- [47] S. Chang, G. D. Kribs, D. Tucker-Smith, N. Weiner, Phys. Rev. **D79**, 043513 (2009). [arXiv:0807.2250 [hep-ph]].
- [48] B. Feldstein, P. W. Graham, S. Rajendran, Phys. Rev. **D82**, 075019 (2010). [arXiv:1008.1988 [hep-ph]].
- [49] A. Falkowski, J. Juknevich, J. Shelton, [arXiv:0908.1790 [hep-ph]].
- [50] J. Kang, M. A. Luty, S. Nasri, JHEP **0809**, 086 (2008). [hep-ph/0611322].
- [51] D. Spier Moreira Alves, S. R. Behbahani, P. Schuster, J. G. Wacker, JHEP **1006**, 113 (2010). [arXiv:1003.4729 [hep-ph]].
- [52] J. L. Feng, Y. Shadmi, Phys. Rev. **D83**, 095011 (2011). [arXiv:1102.0282 [hep-ph]]; J. L. Feng, V. Rentala, Z. 'e. Surujon, [arXiv:1108.4689 [hep-ph]].
- [53] K. R. Dienes, B. Thomas, [arXiv:1106.4546 [hep-ph]].

- [54] K. R. Dienes, B. Thomas, [arXiv:1107.0721 [hep-ph]].
- [55] B. Fields, S. Sarkar, J. Phys. G **G33**, 1 (2006). [astro-ph/0601514].
- [56] E. Komatsu *et al.* [WMAP Collaboration], Astrophys. J. Suppl. **192**, 18 (2011). [arXiv:1001.4538 [astro-ph.CO]].
- [57] J. Hamann, J. Lesgourgues and G. Mangano, JCAP **0803**, 004 (2008) [arXiv:0712.2826 [astro-ph]]; K. Ichikawa, T. Sekiguchi, T. Takahashi, Phys. Rev. **D78**, 083526 (2008). [arXiv:0803.0889 [astro-ph]]; L. P. L. Colombo, E. Pierpaoli and J. R. Pritchard, Mon. Not. Roy. Astron. Soc. **398**, 1621 (2009) [arXiv:0811.2622 [astro-ph]]; S. Joudaki, M. Kaplinghat, [arXiv:1106.0299 [astro-ph.CO]].
- [58] J. L. Feng, M. Kaplinghat, H. -B. Yu, Phys. Rev. Lett. **104**, 151301 (2010). [arXiv:0911.0422 [hep-ph]].
- [59] M. R. Buckley, P. J. Fox, Phys. Rev. **D81**, 083522 (2010). [arXiv:0911.3898 [hep-ph]].
- [60] D. P. Finkbeiner, N. Weiner, Phys. Rev. **D76**, 083519 (2007). [astro-ph/0702587]; D. P. Finkbeiner, T. R. Slatyer, N. Weiner, I. Yavin, JCAP **0909**, 037 (2009). [arXiv:0903.1037 [hep-ph]].
- [61] G. Weidenspointner, C. R. Shrader, J. Knoedlseder, P. Jean, V. Lonjou, N. Guessoum, R. Diehl, W. Gillard *et al.*, [astro-ph/0601673]; J. Knoedlseder, P. Jean, V. Lonjou, G. Weidenspointner, N. Guessoum, W. Gillard, G. Skinner, P. von Ballmoos *et al.*, Astron. Astrophys. **441**, 513-532 (2005). [astro-ph/0506026]; J. Knoedlseder, V. Lonjou, P. Jean, M. Allain, P. Mandrou, J. -P. Roques, G. K. Skinner, G. Vedrenne *et al.*, Astron. Astrophys. **411**, L457-L460 (2003). [astro-ph/0309442].